ELSEVIER

Catalysis Today 45 (1998) 47–54

CATALYSIS TODAY

A study of the effect of sulphation on iron oxide catalysts for methane oxidation

A.S.C. Brown, J.S.J. Hargreaves*, B. Rijniersce

Department of Chemistry and Physics, Catalysis Research Laboratory, Nottingham Trent University, Clifton Lane, Nottingham NG11 8NS, UK

Abstract

Sulphated and non-sulphated iron oxides derived from goethite have been compared as methane oxidation catalysts. It has been observed that sulphation increases surface area, suppresses low temperature total oxidation and enhances the formation of partial oxidation products. Characterisation of these materials prior to activity testing demonstrates that, although transformed into haematite, both exhibit a relic morphology related to that of their precursor and that sulphation causes extensive pitting of crystallites. Analysis of powder X-ray diffraction patterns indicates that the relic morphology is multidomainic and that sulphation increases line widths in relation to the non-sulphated system. The post-reactor sulphated samples were found to have lost crystallinity and both catalysts had changed phase from haematite to maghemite.

Keywords: Iron oxide; Goethite; Sulphation; Methane; Oxidation

1. Introduction

In recent years considerable research attention has been directed towards a number of sulphated metal oxide systems primarily because of their ability to catalyse alkane isomerisation reactions at low temperatures [1–3]. In such systems, it has been demonstrated that the way in which materials are prepared is of crucial importance. Generally, sulphation should be performed using a reagent such as sulphuric acid or ammonium sulphate on the oxide precursor – usually the hydroxide or oxyhydroxide – which is subsequently dried and calcined to yield the active catalyst. The temperature of calcination to produce the most active materials is dependent upon the identity of the oxide and sulphation reagent. It has been proposed that the interesting catalytic properties of such materials is related to the development of ''superacidity'', although this is currently a subject of debate, for example [4,5].

The vast majority of effort to date has been directed towards the isomerisation activity of sulphated zirconia and related materials [6]. In this study, we turn our attention towards the methane oxidation properties of the sulphated iron oxide system. There have been few studies of methane activation on sulphated metal oxides. Lin and Hsu [7] mentioned that their sulphated iron–manganese–zirconia system was able to convert methane to ethane at low temperature, and Murata et al. [8] have recently reported that lithium doped sulphated zirconia is an effective catalyst for oxidative coupling of methane. Our interest in sulphated iron

*Corresponding author.

0920-5861/98/$ – see front matter
PII: S0920-5861(98)00243-0

oxide catalysts arises from the potential of combining acidic centres capable of low temperature hydrocarbon activation with an oxide of pronounced oxidation activity. In this way, it may be possible to oxidise methane under conditions which circumvent the gas-phase chemistry known to limit many systems.

In the following, we describe our preliminary studies on the characterisation and catalytic properties of sulphated iron oxide derived from a well-defined goethite precursor.

2. Experimental

2.1. Catalyst preparation

1. *Goethite precursor.* One hundred ml of a 1 M solution of iron(III) nitrate nonahydrate (Avocado 98+%) prepared using distilled water was added to a polythene screw top bottle. To this, 180 ml of a 5 M sodium hydroxide solution was added with stirring. This solution was then diluted to 500 ml with distilled water and aged in an oven at 70°C for 60 h. The resultant bright yellow precipitate was then filtered and washed with 4 l of distilled water and dried in a vacuum oven at room temperature for two days.
2. *Sulphated iron oxide* (SO_4^{2-}/Fe_2O_3). Two grams of goethite was immersed in 30 ml of 0.5 M sulphuric acid for 30 min. The solution was then filtered and the filtrate was dried at 110°C overnight. The material was then calcined at 550°C for 3 h in static air and was pelleted and sieved (0.6–1.0 mm particles) prior to activity testing.
3. *Iron oxide* (H_2O/Fe_2O_3). This material was prepared in an analogous manner to the sulphated system above except that immersion was performed in distilled water.
4. $\alpha - Al_2O_3$ (Aldrich, 99%) was pelleted and sieved (0.6–1.0 mm particles) prior to activity testing.

2.2. Catalyst testing

Catalyst performance was evaluated in a fixed bed catalytic microreactor operating at 15 bar pressure. A stainless steel jacketed quartz reactor tube (8.5 mm) was used in which 0.75 ml of catalyst was held centrally in the heated zone of a furnace by quartz wool plugs. Methane (Air Products 99%), oxygen (Air Products 99.6%) and helium (Air Products 99.999%) were flowed over the catalyst in the ratio 46–4–12 ml min^{-1} to yield a GHSV of ~4600 h^{-1}. Flow rates were maintained using Brooks thermal mass flow controllers and the pressure was regulated with a Tescom back pressure regulator. All lines downstream of the reactor were trace heated to temperatures in excess of 150°C to prevent condensation of products. Analysis was performed on-line using a Varian Saturn GCMS equipped with a thermal conductivity detector. Megabore Poraplot GS-Q and Megabore GS-Molesieve columns were used to effect the separation.

All experiments were performed in the temperature range 250–550°C using 50°C increments. The reactor was allowed to stabilise for 1 h prior to data collection and the results reported are the means of three analyses made at steady state. The carbon balances of the data were in the range of 97–100% in all cases.

2.3. Catalyst characterisation

Surface area determination was performed by the BET method using nitrogen physisorption.

Transmission electron microscopy was performed using a Jeol 2010 electron microscope, operating at 200 keV. Samples were prepared by sprinkling onto carbon coated copper grids and removing the excess by shaking.

Powder X-ray diffraction studies were performed on a Hiltonbrooks modified Phillips powder diffractometer fitted with a detector monochromator using Cu K_α radiation operating at 40 kV and 20 mA. Samples were prepared by compaction into an aluminium sample holder and were scanned in the range 5–75° 2θ at a step size of 0.05 and 2° min^{-1} counting rate.

3. Results and discussion

Methane oxidation studies have been performed with H_2O/Fe_2O_3, SO_4^{2-}/Fe_2O_3 and α-Al_2O_3 materials (Table 1). α-Al_2O_3 was included in this study because it is considered to be an inert material and therefore indicates the background gas-phase activity which is known to be significant for this reaction [9]. On inspection of the data in Table 1, it is apparent that both iron oxide samples possess activity in excess of

Table 1
Methane oxidation results for α-Al_2O_3, H_2O/Fe_2O_3 and SO_4^{2-}/Fe_2O_3

Sample	Surface area ($m^2\ g^{-1}$)	Temperature (°C)	Conversion (%)		Selectivity (%)[a]			
			CH_4	O_2	CO_2	CO	C_2H_6	CH_3OH
α-Al_2O_3	—	300	—	—	—	—	—	—
		400	—	—	—	—	—	—
		500	0.6	12.9	100	—	—	—
H_2O/Fe_2O_3	13	300	0.1	1.3	100	—	—	—
		400	4.0	73.5	100	—	—	—
		500	5.6	71.9	89	11	—	—
SO_4^{2-}/Fe_2O_3	29	300	—	—	—	—	—	—
		400	0.4	9.2	16	84	—	—
		500	5.9	85.0	32	61	3	4

[a]Based on mol C converted.

the background. In addition a number of interesting effects of sulphation are revealed. Despite increasing the catalyst surface area, sulphation suppressed low temperature total oxidation activity. As temperature was increased further, the conversion observed with the sulphated material increased and surpassed that of its non-sulphated counterpart as would be expected on the basis of relative surface area. At 500°C selective oxidation products were observed. This was possibly a consequence of the differing conversions between these materials. Although the general trends reported for the SO_4^{2-}/Fe_2O_3 are reproducible, it has been found that the performance of this material varies largely between different samples. This phenomenon, which may relate to differences in sulphation level and/or precursor age, is currently being investigated. In their study of sulphated zirconia catalysts, Sarzanini et al. [10] also found that the reproducibility of the sulphation process with sulphuric acid is low and reported that ammonium sulphate was a better reagent in this respect. Farcasiu et al. [11] have recently addressed this problem and have reported an improved preparation method for sulphated zirconia with sulphuric acid. The sulphated iron oxide sample described in the present study has been chosen because it is the most well characterised and exhibits representative catalytic performance.

The effects of sulphation could be due to a number of possible reasons, including selectively blocking total oxidation sites, increasing surface area, differences in phase composition and morphological effects. Accordingly, the iron oxide materials investigated in Table 1 have been characterised by a combination of transmission electron microscopy and powder X-ray diffraction. Fig. 1 presents transmission electron micrographs of the goethite precursor, H_2O/Fe_2O_3 and SO_4^{2-}/Fe_2O_3 materials as prepared. The needle shaped crystals observed in Fig. 1(a) are characteristic of those published in the literature for acicular goethite [12,13]. Fig. 1(b) and Fig. 1(c) show that this general form of morphology was maintained in the H_2O/Fe_2O_3 and SO_4^{2-}/Fe_2O_3 materials, although some growth has occurred along the needle axis (from ca. 0.5 to ca. 1 μm, the surface area of the precursor was 40 $m^2\ g^{-1}$). Powder X-ray diffraction (which is discussed in more detail below) confirmed that the precursor material was goethite and that both Fe_2O_3 systems were haematite. It is known that the morphology of haematite may be related to that of its precursor [12,14]. It is interesting to note that sulphation has caused extensive pitting of the Fe_2O_3 needles. This may, at least partly, explain the surface area differences between the two Fe_2O_3 samples, especially as their needle dimensions appear similar. Previous studies have demonstrated that hole formation can occur in goethite crystals as a result of proton attack at domain boundaries [13,15]. It is therefore proposed that the extensively pitted structure evident in Fig. 1(c) originated from partial dissolution of the goethite precursor during the sulphation procedure.

The powder X-ray diffraction patterns of the H_2O/Fe_2O_3 and SO_4^{2-}/Fe_2O_3 materials are given in Fig. 2.

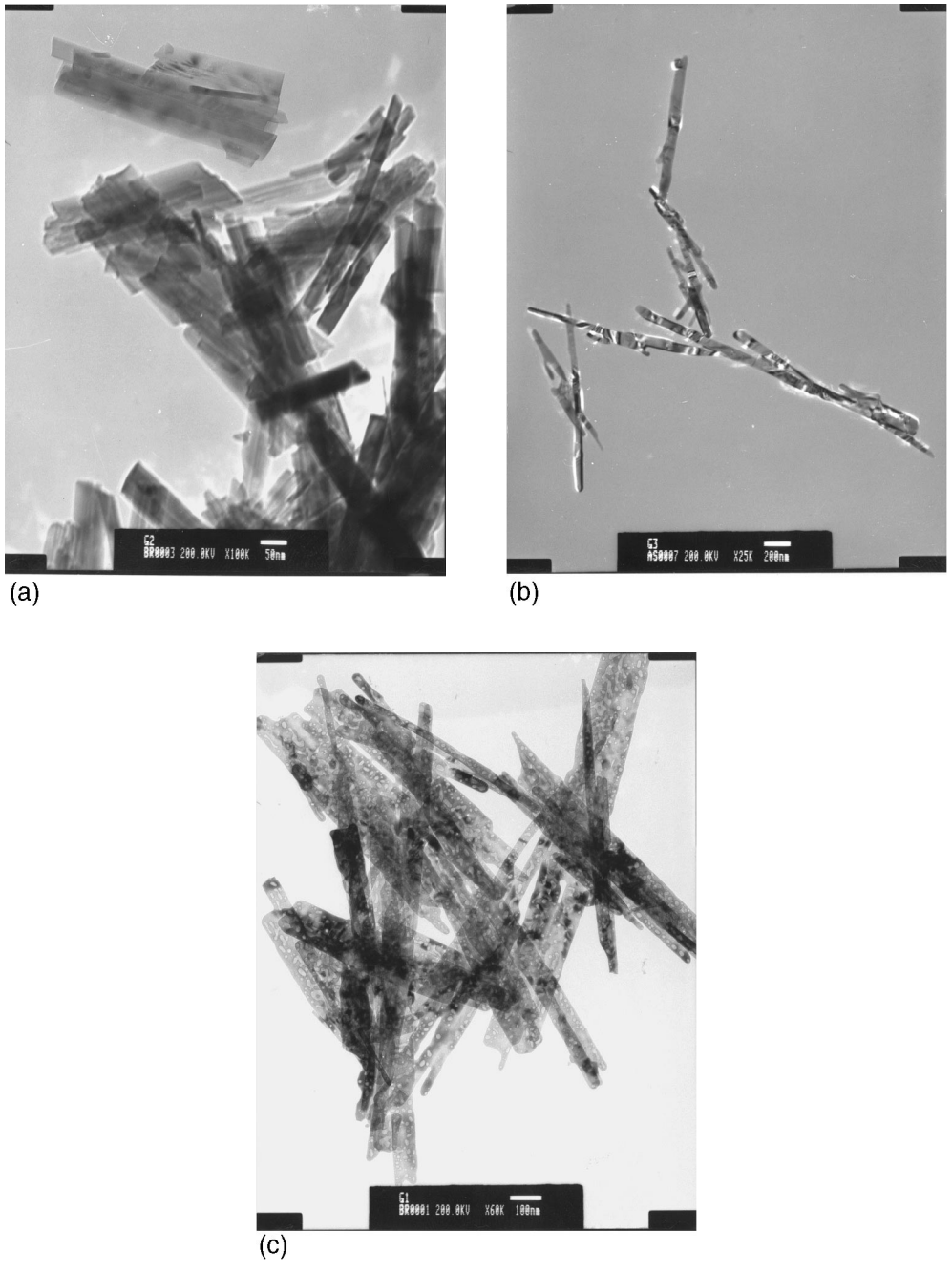

Fig. 1. Transmission electron micrographs of (a) goethite precursor, (b) H_2O/Fe_2O_3 and (c) SO_4^{2-}/Fe_2O_3.

As mentioned above, the forms of both patterns are similar and match to the JCPDS file for haematite (file number 13-534). Inspection of the patterns reveals that there are differences in the full width half maxima of the reflections (Table 2). These are indicative of differences in crystallite (or diffracting domain) size and/or lattice strain effects [16]. Comparison of the apparent crystallite sizes as determined from the Scherrer

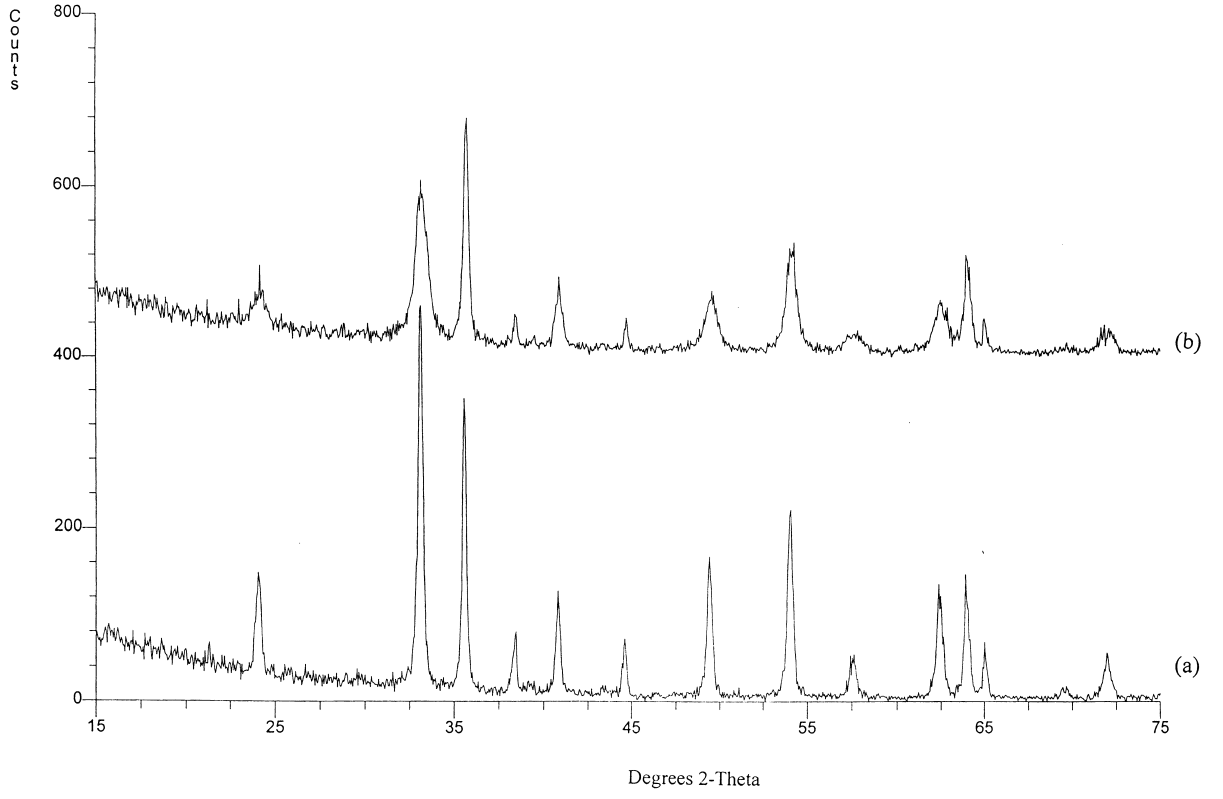

Fig. 2. Powder X-ray diffraction patterns of (a) H_2O/Fe_2O_3 and (b) SO_4^{2-}/Fe_2O_3.

Table 2
Powder X-ray diffraction line widths for H_2O/Fe_2O_3 and SO_4^{2-}/Fe_2O_3 haematite

Reflection	Width (°2θ)[a]	
	H_2O/Fe_2O_3	SO_4^{2-}/Fe_2O_3
(012)	0.350	0.500
(104)	0.300	0.700
(110)	0.200	0.300
(006)	0.150	0.300
(113)	0.300	0.400
(202)	0.300	0.200
(024)	0.250	0.700
(116)	0.300	0.600
(018)	0.400	1.000
(214)	0.200	0.500
(300)	0.200	0.150
(1010)/(119)	0.250	1.000

[a] α_2 stripped.

equation (after α_2 stripping and taking the Scherrer constant as 0.9 radian) with the TEM micrographs indicate large differences with respect to the dimensions of the needles. This indicates that either lattice strain contributed to the reflection width in each case or that the crystallites shown in Fig. 1(b) and Fig. 1(c) are multidomainic. The observation that reflection widths are generally larger for the sulphated material are consistent with its higher surface area. It is probable that the pitting observed in Fig. 1(c) relates to this in that grain boundary regions are disrupted, reducing sintering. Complexation by sulphate, as evidenced in our FTIR studies of the sulphated goethite precursor, may also contribute. Four bands were observed in the v S=O region (1226, 1137, 1077 and 996 cm^{-1}) which can be assigned to sulphate binding with a C_{2v} symmetry [17]. A related study has also reported that sulphate binds to goethite with a C_{2v} symmetry bridging two cations [18]. Sulphate may therefore inhibit domain grain growth by restricting cationic mobility. The transformation of goethite to haematite involves the loss of water and the rearrangement of the cations – the anionic frameworks of these materials are related [12]. Norman et al. [19] have made similar suggestions

for the role of sulphate in stabilising the surface area of zirconia. They have proposed that sulphate binds two cations in a bridging mode which reduces nucleation due to increased separation and thermal stability with respect to OH bridges. Careful comparison of the diffraction patterns/reflection widths in Fig. 2 and Table 2 indicates that, whilst there are similar relative trends, sulphation had anisotropic effects. This can possibly be due to modification of morphology and/or strain and suggests face specific interaction of goethite with sulphuric acid. Previous studies have demonstrated that sulphate exerts a morphological effect on haematite prepared by hydrolysis of ferric solutions [20].

Powder X-ray diffraction analysis has been applied to the iron oxide samples after reaction. It is important to emphasise that the relationship of this study to the data given in Table 1 may be somewhat limited since the catalysts were subsequently exposed to a higher temperature (550°C) than the maximum reported. The diffraction patterns for the samples are shown in Fig. 3. On discharge from the reactor, it was apparent that the crystallinity of the sulphated sample had decreased markedly, and that there were phase changes for both materials. Both samples consisted of maghemite (JCPDS file number 25-1402) which is obviously a consequence of the exposure of the catalysts to reaction atmosphere, since in the temperature range investigated maghemite would be expected to transform to haematite [13]. The major loss of crystallinity for the sulphated system appears to be a consequence of its higher surface area. Again, it was observed that there are differences in reflection full width half maxima and these are reported in Table 3. As was the case for the pre-reactor samples, sulphation had significantly increased the widths of some reflections with respect to those for the non-sulphated samples, again suggesting smaller diffracting domains or introduction of lattice strain.

In summary, it has been found that sulphation of iron oxide prepared from a well defined goethite precursor produces some interesting catalytic and

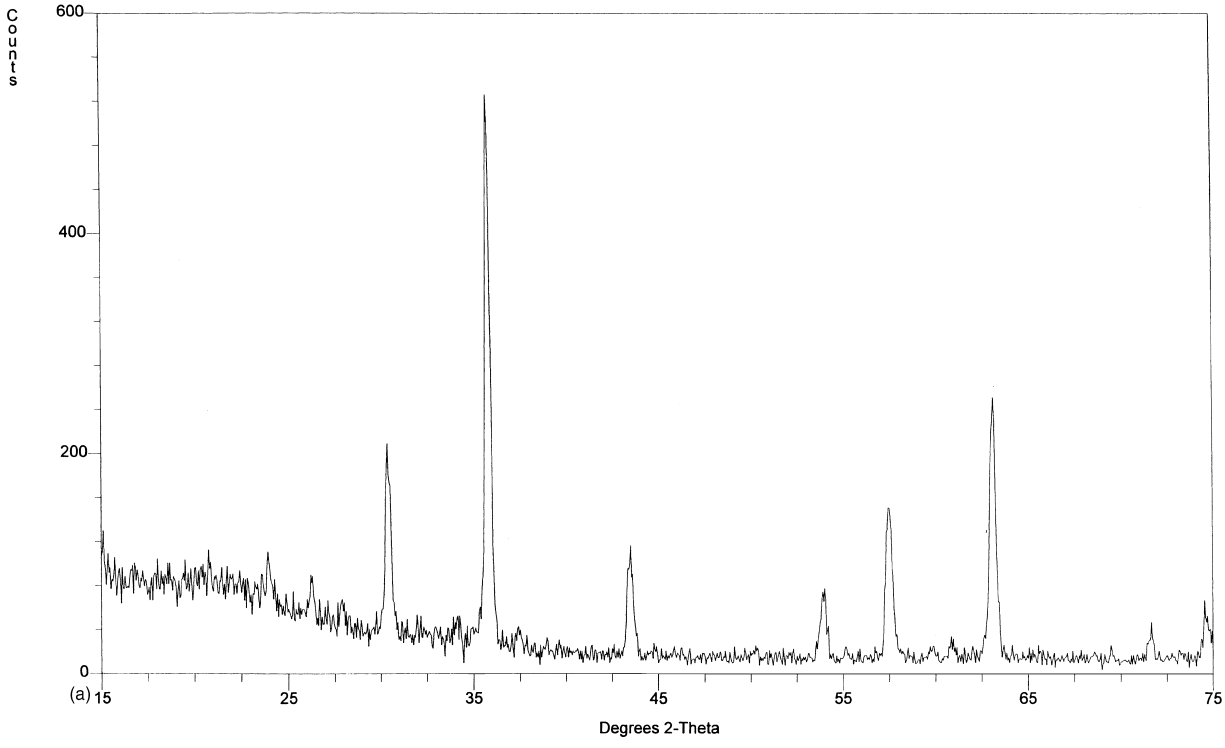

Fig. 3. Powder X-ray diffraction patterns for (a) H_2O/Fe_2O_3 and (b) SO_4^{2-}/Fe_2O_3 after activity testing.

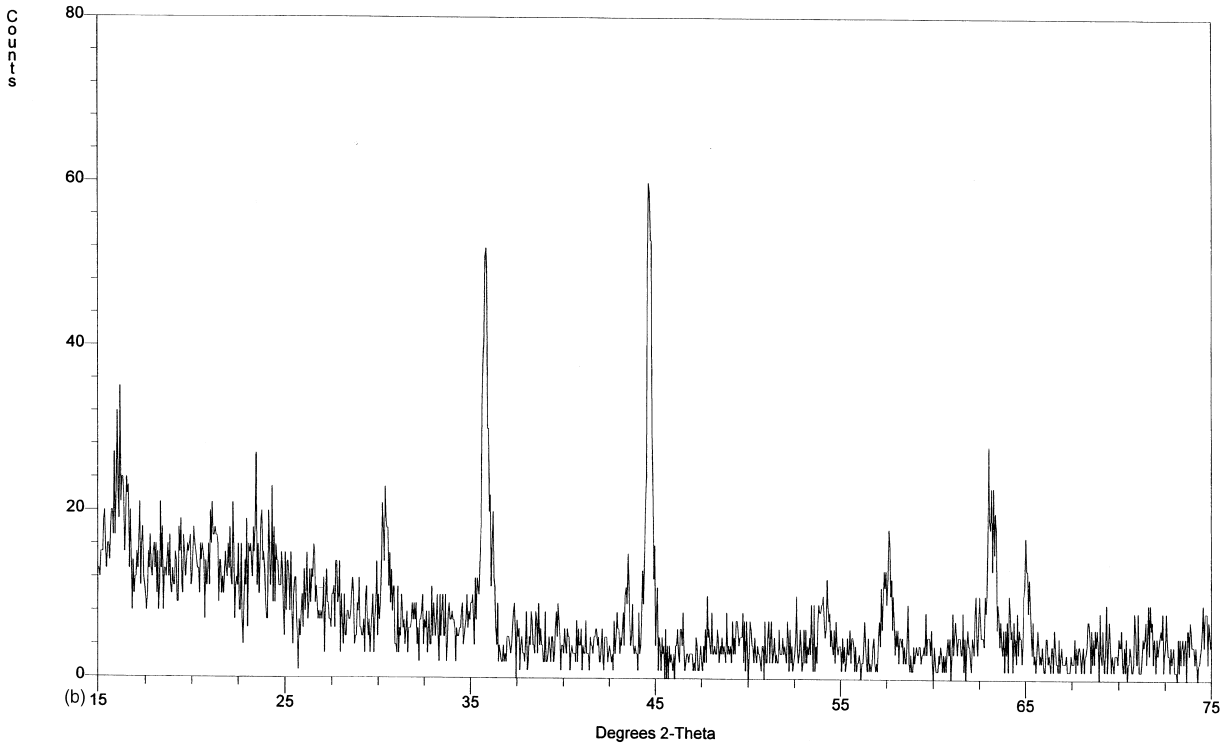

Fig. 3. (*Continued*)

Table 3
Powder X-ray diffraction line widths for post-reactor H_2O/Fe_2O_3 and SO_4^{2-}/Fe_2O_3 maghemite samples

Reflection	Width (°2θ)[a]	
	H_2O/Fe_2O_3	SO_4^{2-}/Fe_2O
(220)	0.150	0.500
(313)	0.200	0.300
(513)	0.350	0.600
(440)	0.350	0.400

[a] α_2 stripped.

structural effects which may be related. Further studies on this system are in progress. In particular, we are investigating the relationship between sulphate content and catalytic performance, whether the observation of partial oxidation products is an intrinsic effect and the morphological/structural effects of sulphation on a series of well-defined FeOOH precursors. The observation that sulphate appears to modify the growth of domains in both the pre- and post-reactor samples may inter-relate to the inhibition of the total oxidation activity. Both processes may occur by the same site specific blocking mechanism. This study clearly indicates that sulphated metal oxide systems are worthy of further attention as oxidation catalysts.

Acknowledgements

It is a pleasure to record our appreciation of the assistance of Drs. David Williams and Michael Crapper (Department of Physics, Loughborough University) for allowing us to use their powder X-ray diffractometer, Mr. D. Lacey (Faculty of Science and Mathematics, Nottingham Trent University), for TEM studies, Professor Richard Joyner and Dr. Michael Stockenhuber (Department of Chemistry and Physics, Nottingham Trent University) for useful discussions.

References

[1] T. Yamaguchi, Appl. Catal. 61 (1990) 1.
[2] A. Corma, Chem. Rev. 95 (1995) 559.
[3] K. Arata, Appl. Catal. A 146 (1996) 3.
[4] D. Farcasiu, A. Ghenciu, J.Q. Li, J. Catal. 158 (1996) 116.
[5] V. Adeeva, J.W. de Hann, J. Janchen, G.D. Lei, V. Schunemann, L.J.M. van de Ven, W.H.M. Sachtler, R.A. van Santen, J. Catal. 151 (1995) 364.
[6] X. Song, A. Sayari, Catal. Rev.-Sci. Eng. 38 (1996) 329.
[7] CH. Lin, C-Y. Hsu, J. Chem. Soc., Chem. Commun. (1992) 1479.
[8] K. Murata, T. Hayakawa, K. Fujita, Chem. Commun. (1997) 221.
[9] T.R. Baldwin, R. Burch, G.D. Squire, S.C. Tsang, Appl. Catal. 74 (1991) 137.
[10] C. Sarzanini, G. Sacchero, F. Pinna, M. Signoretto, G. Cerrato, C. Morterra, J. Mater. Chem. 5 (1995) 353.
[11] D. Farcasiu, Q. Li, S. Cameron, Appl. Catal. A 154 (1997) 173.
[12] U. Schwertmann, R.M. Cornell, Iron Oxides in the Laboratory, VCH, Weinheim, 1991.
[13] R.M. Cornell, U. Schwertmann, The Iron Oxides, VCH, Weinheim, 1996.
[14] C.H. Rochester, S.A. Topham, J. Chem. Soc., Faraday Trans. I (1979) 1073.
[15] R.M. Cornell, A.M. Posner, J.P. Quirk, J. Inorg. Nucl. Chem. 36 (1974) 1937.
[16] R. Delhez, T.H. de Keijser, J.I. Langford, D. Louer, E.J. Mittmeijer, E.J. Sonneveld, in: R.A. Young (Ed.), The Rietveld Method, Oxford Science Publications, Oxford, 1993.
[17] K. Nakamoto, Infrared and Raman Spectra of Inorganic and Co-ordination Compounds, 4th ed., Wiley, New York, 1986.
[18] R.L. Parfitt, R.St.C. Smart, J. Chem. Soc., Faraday Trans. 1 (1977) 796.
[19] C. J. Norman, P.A. Goulding, P.J. Moles, in: M. Hattori, M. Misono, Y. Ono (Eds.), Stud. Surf. Sci. Catal., 90 (1994) 269.
[20] N.J. Reeves, S. Mann, J. Chem. Soc., Faraday Trans. 87 (1991) 3875.